Received: 30 June 2019 | Revised: 19 October 2019 | Accepted: 13 November 2019

DOI: 10.1002/sia.6729

SPECIAL ISSUE ARTICLE

WILEY SURFACE and INTERFACE ANALYSIS

Optimization of SIMS analytical parameters for water content measurement of olivine

Wan-Feng Zhang[1,2] | Xiao-Ping Xia[1] | Takahashi Eiichi[1] | Li Li[1] | Qing Yang[1] | Yan-Qiang Zhang[1] | Ya-Nan Yang[1] | Ming-Liang Liu[3] | Chunkit Lai[4]

[1] State Key Laboratory of Isotope Geochemistry, Guangzhou Institute of Geochemistry, Chinese Academy of Sciences, Guangzhou, China

[2] College of Earth and Planetary Sciences, University of Chinese Academy of Sciences, Beijing, China

[3] Laboratoryof Elemental Analysis, Guangzhou Isotope Testing Technology Co., Ltd, Guangzhou, China

[4] Faculty of Science, Universiti Brunei Darussalam, Gadong, Brunei Darussalam

Correspondence
Xia Xiao-Ping, Guangzhou Institute of Geochemistry, Chinese Academy of Sciences, Guangzhou 510640, China.
Email: xpxia@gig.ac.cn

Funding information
GIGCAS, Grant/Award Number: GIG-GNKF-201601; Guangzhou Municipal Government, Grant/Award Number: 201607020029; National Natural Science Foundation of China, Grant/Award Numbers: 41603045 and 41673010; National Key R&D Program of China, Grant/Award Number: 2018YFA0702600

Secondary ion mass spectrometry (SIMS) has a wide range of applications in Earth Science research, thanks to its high precision and sensitivity, and its capacity in direct insitu micromeasurement. The technique is operated in ultra-high vacuum (UHV) conditions, especially for the measurement of volatiles such as hydrogen, or the water content in nominally anhydrous minerals (NAMs). To minimize the water background and obtain accurate and precise water contents in NAMs (eg, olivine) critical parameters such as presputtering time, field aperture (FA), dynamic transfer on/off, and primary beam current intensity were investigated for a CAMECA IMS 1280-HR system. When the chamber vacuum reaches approximately 2×10^{-9} mbar, we set the DTOS OFF, raster size to 50 μm and primary beam current to 5 nA, and used 2000 μm FA and 170-second presputtering time. Consequently, an approximately 1.2 ppmw water background and 3.6 ppmw limit of detection (LOD) were yielded, from analyzing the San Carlos olivine. Meanwhile, the water content and homogeneity of a range of olivine minerals were characterized for potential use as reference materials for SIMS water content measurement. Olivine water content calibration curve was also established by comparing the Fourier transform infrared (FTIR) results with the SIMS-measured $^{16}O^{1}H^{-}/^{16}O^{-}$ ratios. Accuracy and precision of water content measurement were estimated to be better than approximately 10% in this study.

KEYWORDS

nominally anhydrous minerals (NAMs), olivine reference material, SIMS, water content

1 | INTRODUCTION

Studying the Earth's water budget and the identifying of suitable reservoirs for H (colloquially "water") in the crust and mantle are long-standing problems in geology and have important implications on the planetary evolution as a whole. Determining the water contents in various rocks and minerals is important to understand the volatile recycling processes (including degassing) in the crust and mantle, which are closely linked to the evolution of the Earth's hydrosphere and atmosphere. Nominally anhydrous minerals (NAMs) are a major reservoir of mantle hydrogen, which possibly accommodates all water in the depleted mantle.[1]

Fourier transform infrared (FTIR) spectroscopy is most commonly used to determine the water content and its species in glasses and minerals.[2] It has the capacity to measure low hydrogen abundance and to provide information on hydrogen species with very high special resolution.[3] However, the samples to be analyzed by this technique need to be of such a dimension that allows wafers to be manufactured, typically around 100 μm thick and double polished. This requirement limits the application of FTIR to small-sized samples (<100 μm).[4] Secondary ion mass spectrometry (SIMS) provides insitu micromeasurements of elemental and isotopic compositions in selected millimeter- to centimeter-sized solid sample for almost all elements in nature[5] and is ideal for measuring the water content in

NAMs.[2,4,6,7] Moreover, SIMS can simultaneously yield water content and oxygen isotope compositions, which are essential to trace the origin of water.[2,4] CAMECA IMS f series and Sensitive High Resolution Ion Microprobe-Stable Isotope (SHRIMP-SI) have been preciously used for this purpose, with usually a relatively high background of approximately 10 to 30 ppmw.[3,4,7] This limits its application to NAMs, notably olivine, whose has water content can be as low as 10 ppmw.[1,8,9]

Previous study by Turner et al.[4] showed that a background of approximately 30 ppmw (with vacuum of 7×10^{-9} mbar in sample chamber) can be achieved for large geometry SIMS (SHRIMP-SI). We have further reduced that to approximately 10 ppmw by liquid nitrogen cooling of the sample chamber and by using tin-based alloy for sample mounting in our previous study,[10] which yielded a vacuum of approximately 2×10^{-9} mbar in the chamber. Our previous study (on simultaneous measurement of water content and oxygen isotopes) requires the machine settings to be optimized for high-precision measurement, whereas the opposite may be better for low water content measurement: For instance, dynamic transfer "on" of CAMECA IMS 1280-HR is good for high-precision measurement, whereas "off" is good for low water content measurement. To minimize water background and to obtain more accurate/precise measurements of water contents in olivine, several critical parameters, including presputtering time, field aperture (FA), dynamic transfer on/off, and primary beam current intensity were investigated in this study. Our approach has minimized the water background and limit of detection (LOD) to 1.2 and 3.6 ppmw, respectively, as estimated from the analytical results on San Carlos olivine. We also developed a set of olivine reference materials for water content calibration, which covers a water content range of 1.42 to 70.6 ppmw.

2 | SAMPLES AND ANALYTICAL METHODS

2.1 | Samples

To minimize the background of water, San Carlos olivine (about 1 ppmw H_2O) was selected to optimize the operating settings. And the water content and homogeneity of olivine samples including San Carlos, KLB-1, ICH-30, and Mongok olivine were characterized as potential reference materials. The San Carlos olivine sample was separated from an ultramafic inclusion from Arizona and had been widely used as reference material for oxygen isotope analyses.[11-15] A grain of San Carlos olivine with size of 1 cm^3 was used in this study. KLB-1 olivine sample was from the Kilborne Hole crater in New Mexico. This sample was used as the starting material for the high-temperature/-pressure petrological experiments by Takahashi et al.[16] It represents an undepleted mantle composition, and it is available in large quantities. A grain of 0.5 cm^3 in size was used in this study. ICH-30 olivine sample (size: 0.5 cm^3) is an ultramafic xenolith separated from a spinel lherzolite from the Ichinomegata crater, Oga Peninsula in northeastern Japan.[17,18] Mongok olivine sample is 1 cm^3 in size and was purchased from a mineral store in Burma. No geological information is available about this mineral. Judging from its very MgO-rich composition, Mongok olivine may be crustal metamorphic origin possibly in skarn environment.

2.2 | Analysis method

Major element compositions of the four olivine samples were determined with a JEOL JXA-8100 electron probe microanalyzer (EPMA) at the State Key Laboratory of Isotope Geochemistry, Guangzhou Institute of Geochemistry, Chinese Academy of Sciences (SKLaBIG-GIGCAS), and the conditions are as follows: 15 kV accelerating voltage, 20 nA beam current, and 5 μm beam diameter. The ZAF correction procedure was adopted for data reduction.

Water content of the samples were firstly analyzed by FTIR. Total vacuum-type FTIR microscope by JASCO Company (FT-IR-6100) located at the SKLaBIG-GIGCAS were used. Because of the vacuum system, LOD for H_2O in this system is less than 0.1 ppmw.[19] The samples were cut into tabular rhomboids of 500 to 3000 μm thick and polished on both sides. Samples were heated in an oven at 80°C for at least an hour prior to analysis in order to remove potential surface contaminated water. Inclusion-free and clear olivine from the four samples were analyzed with polarized FTIR spectroscopy. Quantification of water contents in olivine from the four samples was based on the total absorbance normalized to 1 cm thickness, using the calibration factor of Bell et al.[20] for olivine (Fo_{90}) composition. Since the FTIR spectra of olivine exhibit strong anisotropy, single crystals were measured from *X*, *Y*, and *Z* directions using polarized light. *X* and *Y* directions were measured on one plane of the doubly polished single crystals, and *Z* direction was measured on another plane perpendicular to the *X*-*Y* plane. Thickness of the sample was measured by a micrometer. FTIR measurements were repeated on 3 to 5 different points of the same crystal, and the standard deviation (1SD, %) was calculated.

Typically, up to 800 scans were performed for each measurement at 2 cm^{-1} nominal resolution to obtain spectra with a signal to noise ratio of >1000. The method has been described in detail by Sakurai et al.[19]

After FTIR analyses, all the samples were placed on a double-sided adhesive type and enclosed in tin-based alloy, same as the method described by Zhang et al.[10] The alloy mount was photographed under reflected light with an optical microscope and then gold-coated (approximately 30 nm thick) before the SIMS analysis.

The SIMS analysis was performed with a CAMECA IMS 1280-HR at the SIMS laboratory in SKLaBIG-GIGCAS. Before the analysis, the machine (including the sample chamber without the sample mounts) was baked at least 24 hours. After it cools down, the sample mount was transferred into the sample chamber, which was then vacuumed to 5×10^{-9} mbar starting the automatic liquid nitrogen refilling system (generally takes 1-2 hours). Although the IMS 1280-HR had a large chamber, the vacuum could reach an ultimate ultrahigh condition (approximately 2×10^{-9} mbar) when this alloy mount coupled

with the liquid nitrogen cooling technique was used.[10] A Cs^+ primary beam of 4 to 5 nA and diameter of approximately 15 μm, with an impact energy of 10 kV was used to sputter secondary ion from the samples. The size of the analytical area was 30 × 30 μm (15 μm spot size + 15 μm rastering). A normal-incidence electron gun was used to ensure a charged compensation during all measurement sessions. The NEG was carefully tuned to yield a rounded and homogeneous cover with a diameter of approximately 120 μm and a maximum emission current of approximately 1 mA. The nuclear magnetic resonance (NMR) controller was used to stabilize the magnetic field, which provided stability of 5 ppmw over 24 hours.[21] The contrast aperture, the entrance slit, max area, and the exit slit were set at 400, approximately 60, approximately 80, and approximately 173 μm, respectively. The energy slit was set to 50 eV with 5 eV gap. Although we focused on water content measurement, the oxygen isotope compositions were also simultaneously measured with the multicollector system to compare with our previous data[2]. Two Faraday cup detectors, located on L'2 and H1 trolleys with 10^{10} and 10^{11} Ω amplifiers, and an electron multiplier of monocollector were used to measure the $^{16}O^-$, $^{18}O^-$, and $^{16}O^1H^-$, respectively. For $^{16}O^-$ and $^{18}O^-$, 500 mm collector slits were used to yield an approximately 2500 MRP with sufficiently flat plateau, while an approximately 173 μm exit slit was used for electron multiplier to yield an approximately 7000 MRP, in order to obtain a sufficiently flat plateau and separate isobaric interference of $^{17}O^-$ on $^{16}O^1H^-$. Analyses were carried out near the center of the mount to avoid influence by the X-Y effect[11].

3 | OPTIMIZATION OF SIMS PARAMETERS

3.1 | Presputtering time

Sample surface is a large reservoir of water in NAMs as it is easy to be contaminated by deposition of water molecules. Thus, presputtering before the analysis is important for low water content measurement. The target analytical area (30 × 30 μm) is firstly rastered in a bigger size (eg, 50 μm × 50 μm) to remove the gold coating or other surface contamination. When the surface was not sputtered enough, such as when presputtering time 90 seconds, the measured within-spot $^{16}O^1H^-/^{16}O^-$ ratio decreased as the cycle of analyses increased (Figure 1A). The measured $^{16}O^1H^-/^{16}O^-$ ratio of a single spot decreased with increasing presputtering time, and a minimum was reached after 170 seconds (Figure 1B). Therefore, presputtering time was set to be 170 seconds.

3.2 | Field aperture

Redeposition of sputtered materials is another major source of water surface contamination, which can be recognized by a higher OH^- intensity along the margins of the analyzed area.[6] The blanking technique can eliminate this interference in NanoSIMS 50L, which integrate signals only from the predefined inner region of the sputtering area. In IMS 1280-HR, FA has similar function. It is a motorized, continuously variable aperture consisting of two square apertures moving symmetrically in a 45° direction between *X* and *Y*. The FA size is an important parameter to minimize water background. Figure 2 shows that the signal decreased rapidly after FA was activated. When the FA was set to 2000 μm, the measured $^{16}O^1H^-/^{16}O^-$ is remarkably lower than that when FA = 2500 μm, which means that the $^{16}O^1H^-$ signal from the periphery of the analyzed area was blocked. When the FA was set to <2000 μm, there is no discernible variation in $^{16}O^1H^-/^{16}O^-$. Therefore, FA = 2000 μm, which limits the ion optical field of view to a smaller area than the primary beam diameter was selected.

3.3 | Dynamic transfer

The primary rastering system allows the primary beam to be deflected within the sample plane over an area up to 500 μm. A so large field image cannot pass through the FA even at low

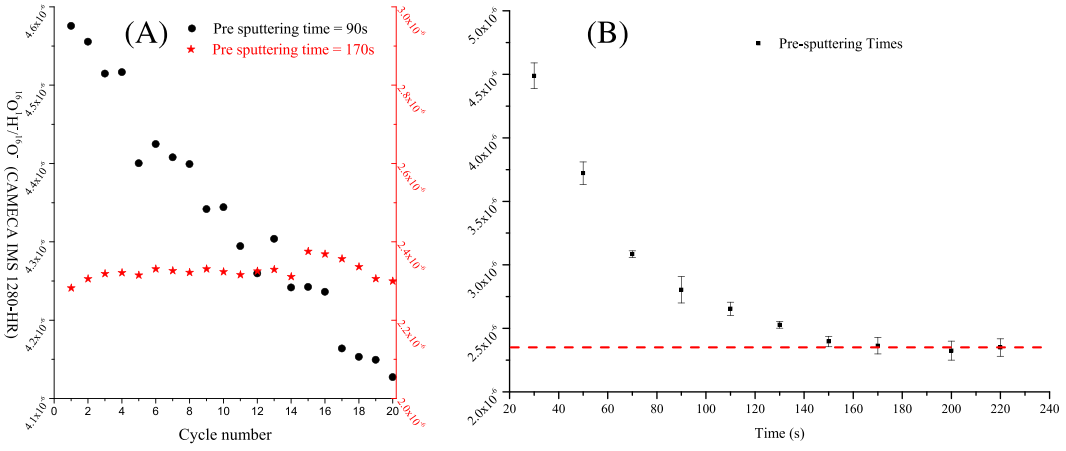

FIGURE 1 Effect of presputtering times on water content measurement: A, typical results (set presputtering time to 90 and 170 s) about the signal in every cycle; B, results of different presputtering time vs $^{16}O^1H^-/^{16}O^-$ ratios

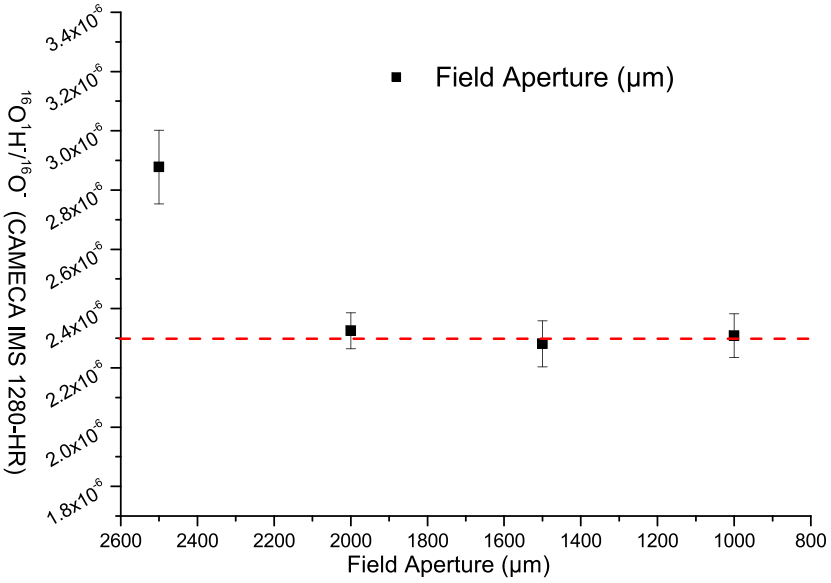

FIGURE 2 Effect of field aperture on water content measurement. The measured $^{16}O^1H^-$ ratios remained constant when the field aperture is smaller than 2000 μm

mass resolution, when the largest FA can be used. The dynamic transfer (DT), basically a deflection device, is synchronized with the primary raster signal to cancel the scanning of the beam at the FA plane, while keeping the cross-over fixed and to collect secondary ions from a large scanned field. It is useful for improving analytical precision as it can cancel topographic effect of the samples and is thus widely used for $^{18}O^-/^{16}O^-$ or $^{30}Si/^{28}Si$ analyses.[22,23] However, how this function affects water content measurement remains unknown. Session (1) in Figure 3 was set to DTOS OFF, while session (2) was set by the DTOS ON. The results clearly show that lower $^{16}O^1H^-/^{16}O^-$ ratios were obtained when DTOS was OFF. Moreover, when DTOS was OFF, a better fitted calibration curve (Adj. R^2 = 0.998 vs 0.981) was yielded (Figure 3). Thus, DTOS was not activated to minimize water background.

3.4 | Intensity of primary beam current

The $^{16}O^1H^-$ signal acquired on NAMs can be divided into two parts. One part is contributed by the surface contamination, and the other by sputtering of the samples. The former is mainly dependent on the vacuum conditions and the latter on the intensity of the primary beam current. Thus, higher primary beam would help to reduce the effect of water background. This relationship has been observed previously when a NanoSIMS 50L was used to measure the water content, which showed a negative correlation between $^1H^-/^{18}O^-$ with primary beam current.[6] To test the performance of CAMECA IMS 1280-HR, the San Carlos olivine was measured using various intensities of the primary beam ranging from 2 to 10 nA. The measured results show a negative correlation between $^{16}O^1H^-/^{16}O^-$ ratios and primary beam currents (Figure 4A). When a log scale was used

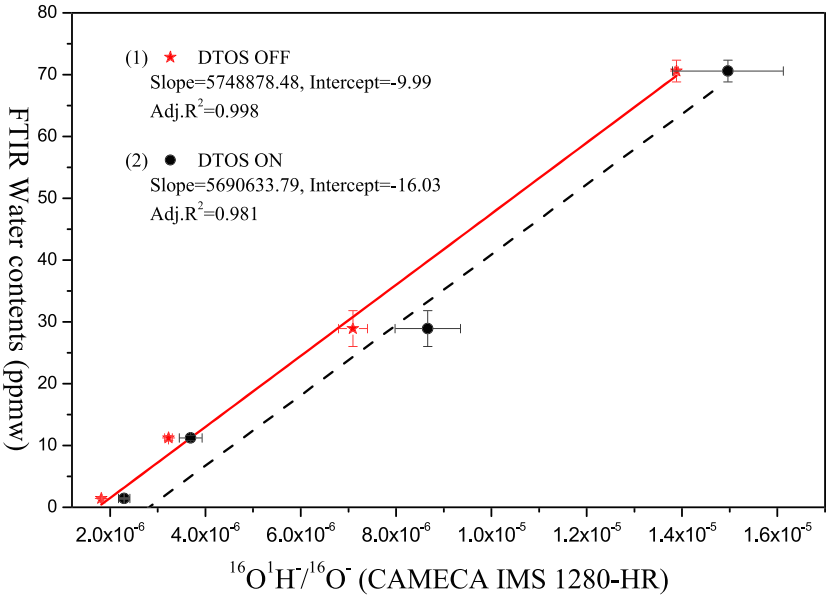

FIGURE 3 Effect of dynamic transfer on water content measurement with the other analytical conditions being held constant

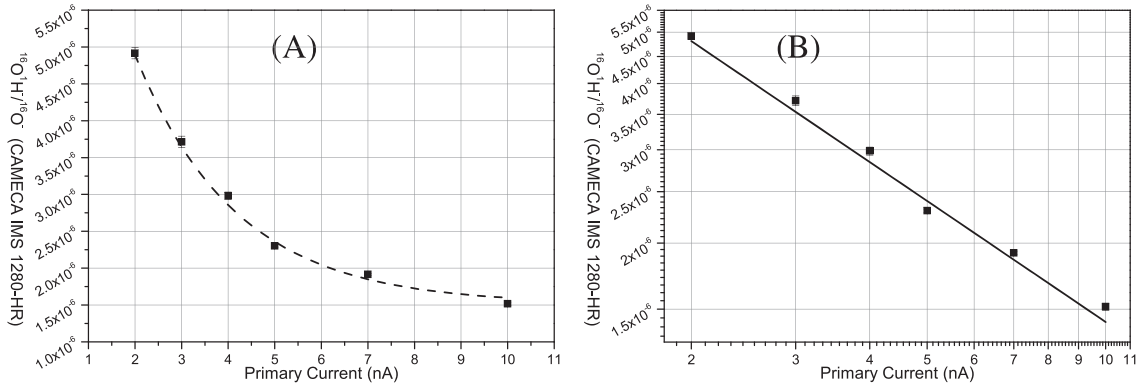

FIGURE 4 Intensity of primary beam current vs $^{16}O^1H^-/^{16}O^-$ ratios measured on San Carlos olivine. The measured $^{16}O^1H^-/^{16}O^-$ ratios are negatively correlated with the primary beam intensity. A, Linear scale and B, log scale

for primary beam, a linear correlation was observed (Figure 4B). The ratio decreased rapidly when the primary beam current increased from 2 to 5 nA. When the primary beam current was over 5 nA, the $^{16}O^1H^-/^{16}O^-$ ratio does not vary much (Figure 4A). Considering that high primary beam current would cause a depth-/charge-related instrumental mass fractionation (IMF),[23] a medium-level primary beam current (4-5 nA) was selected for the water content measurement in NAMs.

4 | RESULTS AND DISCUSSIONS

4.1 | EPMA quantitative analyses

The major element compositions of the four olivine samples were determined by EPMA, and the results were listed in Table 1. The SiO_2 and MgO contents of samples are of 41.87 to 43.17 wt% and from 48.13 to 56.34 wt%, respectively. Intragrain variation is <0.52%, indicating good homogeneity of SiO_2 and MgO contents in these samples. Contents of other elements are generally below 1 wt% (Table 1). The Mg# (100 × Mg/(Mg + Fe)) of the samples (except Mongok: Mg# = 98.98) range from 89.33 to 91.07. Mg# of San Carlos olivine sample ranges from 88.57 to 88.80 with a mean of 88.71, and the mean Mg# of KLB-1 and ICH-30 samples is 89.35 and 90.49, respectively.

4.2 | FTIR results

FTIR spectra were obtained with a polarized transmission model from three mutually perpendicular planes of the olivine blocks (Figure 5). The spectra with similar shapes and an integrated area variation within 10% (1SD) were considered as homogeneous, and their average value was used to calculate the total water content. The FTIR analytical results and calibrated water content values for all the olivine samples were shown in Table 2 and Figure 5. All the analyzed samples show highly oriented absorption bands at 3700 to 3300 cm^{-1}. The background was subtracted using a spline curve fitted to the spectra and all the peaks between 3700 and 3200 cm^{-1} were integrated. As all spectra in the olivine crystals are similar irrespective of total absorbance, the water site is the same regardless of its content. However, the absorbance of the Mongok olivine was markedly different from that of the other three olivine samples with an absorbance at 3595, 3612, and 3675 cm^{-1}, which may be attributed to differences in the hydrogen substitution mechanism in the olivine lattice, led by differences in pressure, temperature, and/or composition. The water

TABLE 1 Electron probe microanalyzer (EPMA) results

Sample		SiO_2	FeO*	MnO	NiO	CaO	MgO	Total	Fo
San Carlos	Mean	41.32	8.80	0.13	0.36	0.06	49.89	100.63	91.07
	Range	41.10-41.51	8.64-8.91	0.08-0.18	0.34-0.38	0.05-0.07	49.48-50.07	100.50-100.84	90.90-91.25
KLB-1	Mean	41.22	10.41	0.14	0.35	0.06	48.43	100.68	89.33
	Range	40.87-41.42	10.07-10.70	0.12-0.17	0.28-0.41	0.06-0.07	48.13-48.85	100.50-101.09	89.00-89.72
ICH-30	Mean	41.47	9.22	0.12	0.36	0.05	49.31	100.58	90.59
	Range	41.33-41.68	8.81-9.38	0.09-0.16	0.31-0.39	0.04-0.05	48.99-49.69	100.25-100.80	90.43-91.03
Mongok	Mean	42.86	1.04	0.02	0.02	0.02	55.90	99.88	98.98
	Range	42.57-43.17	0.98-1.10	0.00-0.06	0.00-0.04	0.01-0.04	55.23-56.34	99.42-100.54	98.90-99.04

Note. Fo = 100 * Mg/(Mg + Fe). FeO*: all Fe as Fe^{2+}.

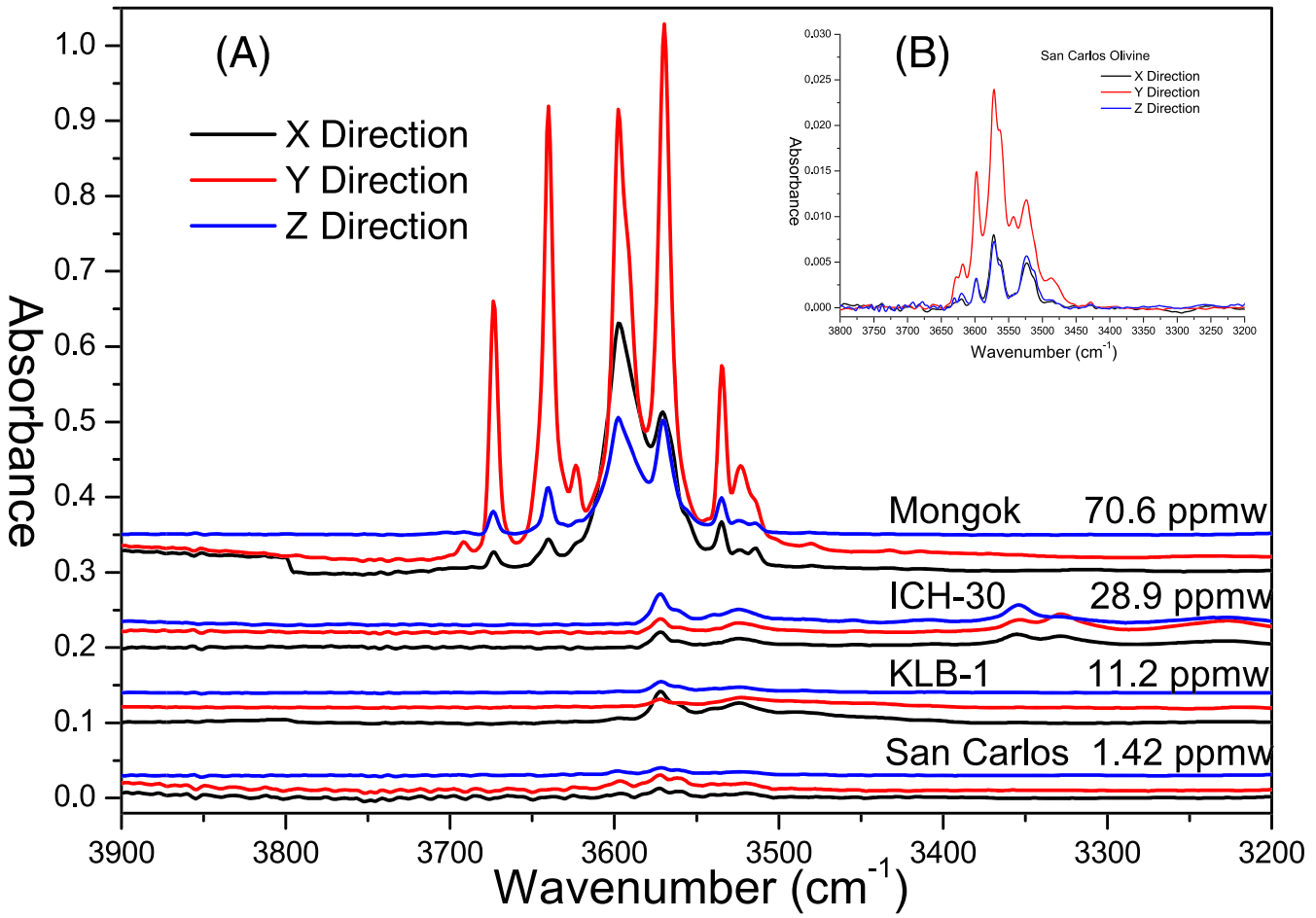

FIGURE 5 Fourier transform infrared (FTIR) spectra of (A) the olivine samples and (B) the San Carlos olivine sample

TABLE 2 Fourier transform infrared (FTIR) results

Sample	A_x,[a] cm^{-2}	A_y, cm^{-2}	A_z, cm^{-2}	Thickness[a,b]	Thickness[b,c]	H_2O, ppmw	SD, %
San Carlos	1.45	0.38	0.39	0.289	0.216	1.42	6.5
KLB-1	1.31	2.84	0.71	0.098	0.042	11.2	3.5
ICH-30	2.8	3.7	3.5	0.071	0.057	28.9	10
Mongok	13.9	33.1	7.78	0.166	0.084	70.6	2.5

[a]*A* is the integrated area, which has been normalized to 1 cm thickness.

[b]Thickness of olivine in directions *X* and *Y*. The unit is mm.

[c]Thickness of olivine in direction *Z*. The unit is mm.

contents were calculated to be 1.42 ppmw for San Carlos, 11.20 ppmw for KLB-1, 28.90 ppmw for ICH-30, and 70.60 ppmw for Mongok.

4.3 | SIMS results

Four olivine samples were analyzed through the optimized conditions in three sessions at different time. Detailed $^{16}O^1H^-/^{16}O^-$ results are listed in Table S1 and summarized in Table 3. The average of measured $^{16}O^1H^-/^{16}O^-$ ratios for the San Carlos, KLB-1, ICH-30, and Mongok are 2.31×10^{-6}, 3.68×10^{-6}, 8.64×10^{-6}, and 1.49×10^{-5}, respectively.

Oxygen isotope analyses of the KLB-1, ICH-30 and Mongok during this study were referenced to San Carlos olivine, for which a $\delta^{18}O$ value of 5.27 ± 0.10‰ (reference to SMOW) is assumed based on published values.[14,15] The average normalized $\delta^{18}O$ value for KLB-1, ICH-30, and Mongok is 5.11 ± 0.42 (2SD), 5.16 ± 0.44 (2SD), and 24.52 ± 0.51 (2SD), respectively. It is noteworthy that the $\delta^{18}O$ value (24.52 ± 0.51, 2SD) for the Mongok olivine is much higher than that for mantle. The petrogenesis for such high value of $\delta^{18}O$, high Fo

TABLE 3 Summary of SIMS results

Sample Name	Session (1)[a]					Session (2)[b]					Session (3)[c]					All Data				
	Average				Calibrated Water Content[d]					Calibrated Water Content[f]		Average			Calibrated Water Content[g]		Average			
	$^{16}O^1H^-/^{16}O^-$	2SD, %	$\delta^{18}O$	2SD, ‰	H_2O, ppm	2SD[e]	$^{16}O^1H^-/^{16}O^-$	2SD, %	$\delta^{18}O$	2SD, ‰	H_2O, ppm	2SD[e]	$^{16}O^1H^-/16O^-$	2SD, %	$\delta^{18}O$	2SD, ‰	H_2O, ppm	2SD[e]	$^{16}O^1H^-/^{16}O^-$	2SD, ‰	$\delta^{18}O$	2SD[e]
San Carlos	2.30×10^{-6}	10.32	5.27	0.50	1.05	−14.98	2.29×10^{-6}	10.33	5.27	0.38	1.14	−10.94	2.49×10^{-6}	3.13	5.27	0.53	1.67	8.09	2.31×10^{-6}	9.84	5.27	0.47
KLB-1	3.69×10^{-6}	12.9	4.93	0.51	8.40	−14.29	3.69×10^{-6}	12.9	4.73	0.52	8.58	−13.25	3.63×10^{-6}	8.81	5.66	0.22	7.67	−18.71	3.68×10^{-6}	12.02	5.02	0.76
ICH-30	8.66×10^{-6}	15.84	4.78	0.49	34.70	9.12	8.47×10^{-6}	13.68	4.79	0.47	34.00	8.11	8.72×10^{-6}	0.87	5.92	0.35	34.40	8.69	8.64×10^{-6}	13.9	4.97	0.98
Mongok	1.50×10^{-5}	12.68	24.76	0.61	68.20	−1.73	1.50×10^{-5}	15.5	24.48	0.27	68.60	−1.44	1.52×10^{-5}	1.81	24.31	0.63	68.50	−1.51	1.49×10^{-5}	11.92	24.64	0.67

Abbreviations: FTIR, Fourier transform infrared; SIMS, secondary ion mass spectrometry.

[a]Session (1) analyzed in 16 July 2018.

[b]Session (2) analyzed in 28 July 2018.

[c]Session (3) analyzed in 30 May 2019.

[d]The result calculated by calibration line (1).

[e]2SD is calculated as (H_2O calibrated − H_2O FTIR)/(H_2O calibrated + H_2O FTIR) × 50% × 2. Negative error means that calibrated SIMS results are less than those of FTIR.

[f]The result calculated by calibration line (2).

[g]The result calculated by calibration line (3).

(99.00), and high water content (70.6 ppm) for this sample remains unknown but suggesting its crustal metamorphic origin.

4.4 | Water content calibration

The SIMS analyzed $^{16}O^1H^-/^{16}O^-$ ratios were compared with their water content data obtained by FTIR in this study to establish the calibration curve. The equation for the water content calibration curves ($[H_2O] = a \times [^{16}O^1H^-/^{16}O^-] + b$) were defined (Figure 6). Three analytical sessions were performed at different times and the results were shown in Figure 6. All the sessions have had similar calibration line, carried out at different times and with different tuning parameters. The values of a are 5.28×10^6, 5.30×10^6, and 5.26×10^6, respectively, with an average of 5.28×10^6. Meanwhile, the b values are −11.10, −11.02, and −11.41, respectively, with an average of −11.17. The slope, intercept, and adjusted R^2 of the calibration lines established at different times were largely similar. This indicates good stability of the analytical method.

4.5 | Analytical precision and accuracy

The analytical precision was evaluated as the internal precision of within-spot analysis (2SE) and external precision (reproducibility) of spot-to-spot analysis (2SD). Internal precision of a single spot analysis (for $^{16}O^1H^-/^{16}O^-$) was determined by the reproducibility of data cycles for one analytical spot (standard error of the mean), which ranges generally from <0.1% to 1.0% (2SE) and follow the Poisson error theoretical trend (Figure 7 and Table S1). One spot of KLB-1, three spots of Mongok olivine (three of 30 spots) and most spots of ICH-30 (17 out of 30 spots) had low precision beyond three times of Poisson theoretical error. Previous studies[17,18] have shown that ICH-30 is heterogeneous with many minute fluid inclusions and records very complex thermal history prior to its final entrapment by the host andesitce magma. Thus, we interpreted that such large errors are probably related to the microinclusions, which are too fine to be detected by transmissive/reflective spectral imaging.

The external precisions of $^{16}O^1H^-/^{16}O^-$ are all better than 8% and can be better than 1% (2SD, session (3) except ICH-30, Figure 8 and Table 3). The external precision is mainly controlled by the stability of primary beam, the vacuum condition of the chamber, and the heterogeneity of the samples. As shown in Figure 8, there is no significant correlation between the primary beam stability and the $^{16}O^1H^-/^{16}O^-$ external precision, which indicates that the influence of the primary beam variation negligible. Although ICH-30 yielded similar external precision to the other three olivines in sessions (1) and (2), its external precision in session (3) is clearly lower than those of the other three. Considering its low internal precision and complex thermal history, we suggested that the heterogeneity of the sample ICH-30 likely responsible for such low external precision. The remarkable difference of external precisions between different sessions can only be imputed to the unstable vacuum of the sample chamber, although no variation has been recorded for (data not shown).

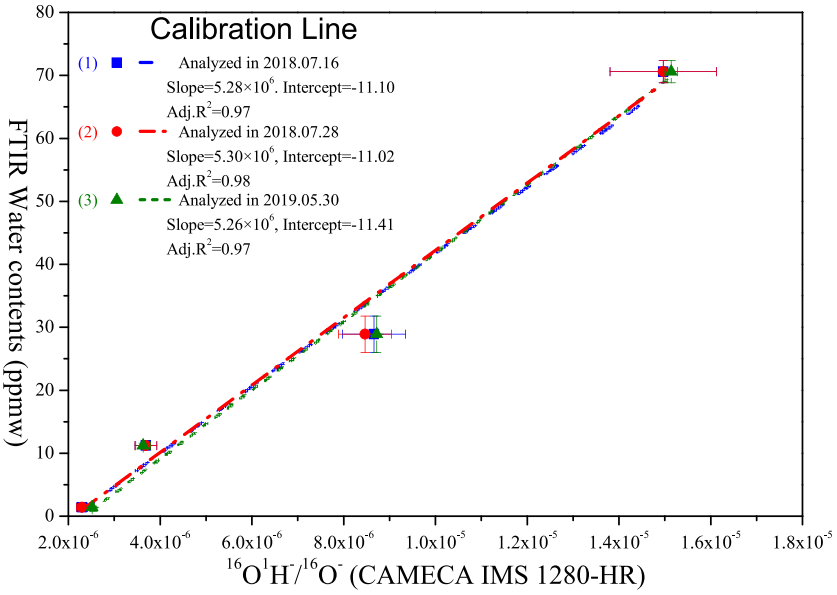

FIGURE 6 Water content calibration curve for secondary ion mass spectrometry (SIMS) olivine analyses

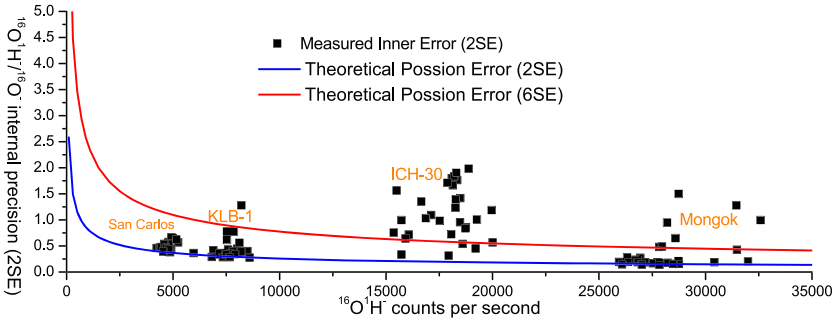

FIGURE 7 Internal precision of SIMS water content analyses for olivine

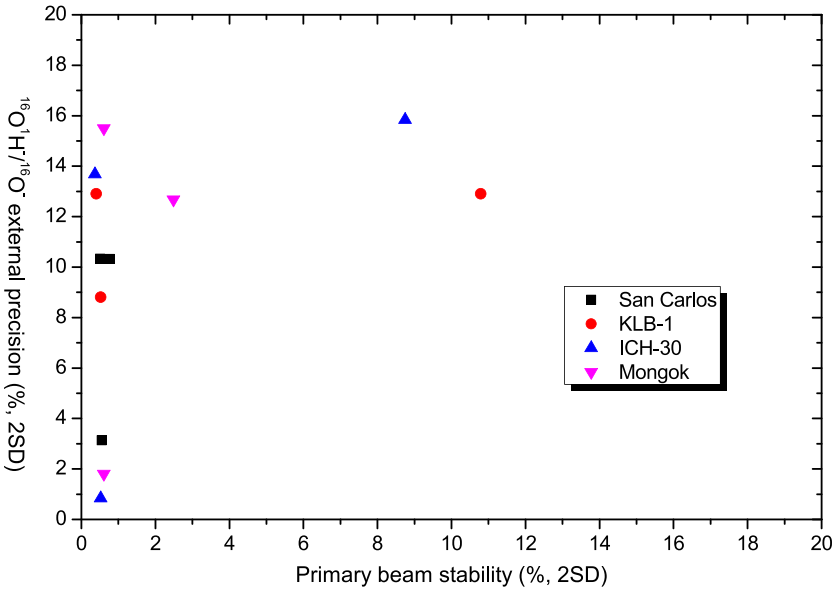

FIGURE 8 Theoretical error and within-spot measured error versus the signal intensity

The internal and external precision of oxygen isotope measurements of San Carlos olivine is <0.41‰ (2SE) and <0.53‰ (2SD), respectively. We noted that both of them are marginally higher in the San Carlos olivine, while 1.5 to 2 times in the other three olivine samples than that of normal oxygen measurement (<0.32‰, 2SE and <0.30‰, 2SD)[24] or simultaneously high-precision measurement of water content and oxygen isotope (0.40‰, 2SE and 0.40‰, 2SD).[2]

To assess the analytical errors, all the olivine samples were treated as unknown to be calibrated using the calibration curves established in this study, and the results were listed in Table S1 and summarized in Table 3. The final error of each spot in Table S1 was calculated by quadratic addition of the uncertainty of the calibration line and the SIMS-measured internal precision of each spot. Uncertainty of the calibration line was evaluated as the average of the difference between the calibrated SIMS water contents and the FTIR results, which range from <1 to 9.35% (1SD). This difference is taken as the accuracy of SIMS water content measurement. Therefore, the accuracy of the water content measurement was estimated to be better than approximately 10% (1SD).

4.6 | Background and LOD for SIMS measurement

Background and LOD can be evaluated based on 2SD and 6SD of background measurement.[25] It is difficult to find a completely water-free sample for background measurement and the zircon 91500 (used as "dry zircon" by De Hoog et al[25]) was reported to contain 56 ppmw water.[2] As earlier work and this study indicated that San Carlos olivine contains about 1 ppmw water,[26] and we took that as "dry" and calculated its 2SD and 6SD for background and LOD evaluation (for the analytical procedure established in this study), which yielded 1.2 and 3.6 ppmw, respectively.

5 | CONCLUSIONS

The background of water content measurement by SIMS is closely related to the vacuum condition, the FA size, the primary beam current, and the presputtering time. The minimum water background (1.2 ppmw) is achieved when the chamber is vacuumed to approximately 2×10^{-9} mbar, DTOS is turned OFF, and a 5 nA primary beam current, 2000 μm FA, and 170-second presputtering time by a IMS 1280-HR is adopted. The water content and homogeneity of four olivine samples including San Carlos were characterized for use as potential reference materials for SIMS water content measurement, which covers a water content range from 1.42 to 70.6 ppmw. Olivine water content calibration curve has been established by comparing the FTIR results with the SIMS-measured $^{16}O^{1}H^{-}/^{16}O^{-}$ ratios on four standard samples. The accuracy of water content measurement by SIMS is estimated to be below approximately 10% in this study.

ACKNOWLEDGMENTS

We thank Zexian Cui for his support in sample preparation and Linli Chen (Guangzhou Institute of Geochemistry) for helping with the EPMA test. This study was funded by the National Key R&D Program of China (2018YFA0702600), the National Natural Science Foundation of China (41673010 and 41603045), the Guangzhou Municipal Government (201607020029), and GIGCAS (GIG-GNKF-201601). This is contribution No. IS-2741 from GIGCAS.

CONFLICT OF INTEREST

There are no conflict of interest to declare.

ORCID

Wan-Feng Zhang https://orcid.org/0000-0001-6481-6162
Xiao-Ping Xia https://orcid.org/0000-0002-3203-039X
Chunkit Lai https://orcid.org/0000-0003-2245-4014

REFERENCES

1. Bell DR, Rossman GR. Water in Earth's mantle—the role of nominally anhydrous minerals. *Science*. 1992;255:1391-1397.
2. Xia X, Cui Z, Li W, et al. Zircon water content: reference material development and simultaneous measurement of oxygen isotopes by sims. *J Anal Atom Spectrom*. 2019;34(6):1088-1097.
3. Koga K, Hauri E, Hirschmann M, Bell D. Hydrogen concentration analyses using SIMS and FTIR: comparison and calibration for nominally anhydrous minerals. *Geochem Geophys Geosyst*. 2003;4:1-20.
4. Turner M, Ireland T, Hermann J, et al. Sensitive high resolution ion microprobe-stable isotope (SHRIMP-SI) analysis of water in silicate glasses and nominally anhydrous reference minerals. *J Anal Atom Spectrom*. 2015;30:1706-1722.
5. Peres P, Kita NT, Valley JW, Fernandes F, Schuhmacher M. New sample holder geometry for high precision isotope analyses. *Surf Interface Anal*. 2013;45:553-556.
6. Hu S, Lin Y, Zhang J, Hao J, Yang W, Deng L. Measurements of water content and D/H ratio in apatite and silicate glasses using a nanoSIMS 50 L. *J Anal At Spectrom*. 2015;30:967-978.
7. Hauri E, Wang J, Dixon JE, King PL, Mandeville C, Newman S. SIMS analysis of volatiles in silicate glasses: 1. Calibration, matrix effects and comparisons with FTIR. *Chem Geol*. 2002;183:99-114.
8. Peslier AH, Bizimis M, Matney M. Water disequilibrium in olivines from hawaiian peridotites: recent metasomatism, h diffusion and magma ascent rates. *Geochim Cosmochim Ac*. 2015;154:98-117.
9. Peslier AH, Woodland AB, Bell DR, Lazarov M. Olivine water contents in the continental lithosphere and the longevity of cratons. *Nature*. 2010;467:78-81.
10. Zhang W, Xia X, Zhang Y, Peng T, Yang Q. A novel sample preparation method for ultra-high vacuum (UHV) secondary ion mass spectrometry (SIMS) analysis. *J Anal Atom Spectrom*. 2018;33:1405-1590.
11. Kita NT, Ushikubo T, Fu B, Valley JW. High precision sims oxygen isotope analysis and the effect of sample topography. *Chem Geol*. 2009;264:43-57.
12. Guo F, Guo J, Wang C, et al. Formation of mafic magmas through lower crustal AFC processes—an example from the Jinan gabbroic intrusion in the North China Block. *Lithos*. 2013;179:157-174.
13. Scicchitano MR, Rubatto D, Hermann J, et al. In situ oxygen isotope determination in serpentine minerals by ion microprobe: reference materials and applications to ultrahigh-pressure serpentinites. *Geostand Geoanal Res*. 2018;42:459-479.
14. Eiler JM, Farley KA, Valley JW, Stolper EM, Hauri EH, Craig H. Oxygen-isotope evidence against bulk recycled sediment in the mantle sources of Pitcairn Island lavas. *Nature*. 1995;377:138-141.
15. Ahn I, Lee JI, Kusakabe M, Choi B. Oxygen isotope measurements of terrestrial silicates using a CO_2-laser BrF_5 fluorination technique and the slope of terrestrial fractionation line. *Geosci J*. 2012;16:7-16.
16. Takahashi E. Melting of a dry peridotite KLB-1 up to 14 Gpa—implications on the origin of peridotitic upper mantle. *J Geophys Res Solid Earth*. 1986;91:9367-9382.

17. Takahashi E. Genesis of calc-alkali andesite magma in a hydrous mantle crust boundary—petrology of lherzolite xenoliths from the Ichinomegata crater, Oga Peninsula, northeast Japan. 2. *J Volcanol Geotherm Res*. 1986;29:355-395.
18. Takahashi E. Thermal history of iherzolite xenoliths. 1. Petrology of iherzolite xenoliths from the Ichinomegata crater, Oga Peninsula, northeast Japan. *Geochim Cosmochim Ac*. 1980;44:1643-1658.
19. Sakurai M, Tsujino N, Sakuma H, Kawamura K, Takahashi E. Effects of al content on water partitioning between orthopyroxene and olivine: implications for lithosphere–asthenosphere boundary. *Earth Planet Sc Lett*. 2014;400:284-291.
20. Bell DR, Rossman GR, Maldener J, Endisch D, Rauch F. Hydroxide in olivine: a quantitative determination of the absolute amount and calibration of the IR spectrum. *J Geophys Res Solid Earth*. 2003;108:8.1-8.8.
21. Li X, Liu Y, Li Q, Guo C, Chamberlain KR. Precise determination of phanerozoic zircon Pb/Pb age by multicollector SIMS without external standardization. *Geochem Geophys Geosyst*. 2009;10:1-21.
22. Tang G, Li X, Li Q, Liu Y, Ling X, Yin Q. Deciphering the physical mechanism of the topography effect for oxygen isotope measurements using a Cameca IMS-1280 SIMS. *J Anal At Spectrom*. 2015;30:950-956.
23. Liu Y, Li X, Tang G, et al. Ultra-high precision silicon isotope microanalysis using a Cameca IMS-1280 SIMS instrument by eliminating the topography effect. *J Anal Atom Spectrom*. 2019;34:906-914.
24. Yang Q, Xia X, Zhang W, et al. An evaluation of precision and accuracy of SIMS oxygen isotope analysis. *Solid Earth Sci*. 2018;3(3):81-86.
25. De Hoog JCM, Lissenberg CJ, Brooker RA, Hinton R, Trail D, Hellebrand E. Hydrogen incorporation and charge balance in natural zircon. *Geochim Cosmochim Ac*. 2014;141:472-486.
26. Aubaud C, Withers AC, Hirschmann MM, et al. Intercalibration of FTIR and SIMS for hydrogen measurements in glasses and nominally anhydrous minerals. *Am Mineral*. 2007;92:811-828.

SUPPORTING INFORMATION

Additional supporting information may be found online in the Supporting Information section at the end of the article.

How to cite this article: Zhang W-F, Xia X-P, Eiichi T, et al. Optimization of SIMS analytical parameters for water content measurement of olivine. *Surf Interface Anal*. 2020;52:224–233. https://doi.org/10.1002/sia.6729